Available online at www.sciencedirect.com
ScienceDirect
Journal of Molecular Structure 873 (2008) 46–60
Journal of MOLECULAR STRUCTURE
www.elsevier.com/locate/molstruc

Novel compounds of 4-amino-1,2,4-triazole with dicarboxylic acids – crystal structures, vibrational spectra and non-linear optical properties

Irena Matulková [a,*], Ivan Němec [a], Karel Teubner [a], Petr Němec [b], Zdeněk Mička [a]

[a] Charles University in Prague, Faculty of Science, Department of Inorganic Chemistry, Hlavova 8, 128 40 Prague 2, Czech Republic
[b] Charles University in Prague, Faculty of Mathematics and Physics, Department of Chemical Physics and Optics, Ke Karlovu 3, 121 16 Prague 2, Czech Republic

Received 1 December 2006; received in revised form 28 February 2007; accepted 3 March 2007
Available online 12 March 2007

Abstract

Three novel 4-amino-1,2,4-triazole compounds with oxalic, succinic and adipic acids have been prepared and X-ray structural analysis has been carried out. The organic salt 4-amino-1,2,4-triazol-1-ium hydrogen oxalate crystallizes in the monoclinic space group $P2_1$, $a = 3.7280(2)$, $b = 18.349(1)$, $c = 4.9680(4)$ Å, $\beta = 101.134(5)°$, $V = 333.44(4)$ Å^3, $Z = 2$, $R = 0.0284$ for 1328 observed reflections. The crystal structure consists of periodically alternating layers (parallel to a axis) formed by chains of hydrogen oxalate anions connected by strong O–H···O hydrogen bonds. The layers are interconnected by 4-amino-1,2,4-triazol-1-ium cations via N–H···O hydrogen bonds.

The addition compound 4-amino-1,2,4-triazole–succinic acid (1:1) crystallizes in the monoclinic space group $P2_1/c$, $a = 11.8130(5)$, $b = 5.0690(3)$, $c = 16.5280(5)$ Å, $\beta = 117.285(3)°$, $V = 879.58(7)$ Å^3, $Z = 4$, $R = 0.0352$ for 1701 observed reflections. The crystal structure is formed by zig-zag chains (parallel to b axis) of 4-amino-1,2,4-triazole molecules, connected by N–H···N hydrogen bonds, and isolated molecules of succinic acid which interconnect these chains by O–H···N and N–H···O hydrogen bonds.

The addition compound 4-amino-1,2,4-triazole–adipic acid (2:1) crystallizes in the monoclinic space group $P2_1/c$, $a = 6.3610(3)$, $b = 8.0580(2)$, $c = 14.8750(5)$ Å, $\beta = 104.072(2)°$, $V = 739.57(5)$ Å^3, $Z = 2$, $R = 0.0487$ for 1793 observed reflections. The crystal structure consists of pairs of parallel linear chains (mediated by N–H···N hydrogen bonds) of 4-amino-1,2,4-triazole molecules that are interconnected by isolated adipic acid molecules via O–H···N and N–H···O hydrogen bonds. Neighbouring chains, which are parallel to a axis, do not exhibit any H-bond contact between each other.

The FTIR and FT Raman spectra of all three compounds were recorded, calculated and discussed.

Quantitative measurements of second harmonic generation of powdered 4-amino-1,2,4-triazol-1-ium hydrogen oxalate at 800 nm were performed and a relative efficiency of 38% (compared to KDP) was observed.

Keywords: 4-Amino-1,2,4-triazole; 4-Amino-1,2,4-triazol-1-ium chloride; 4-Amino-1,2,4-triazol-1-ium hydrogen oxalate; 4-Amino-1,2,4-triazole–succinic acid (1:1); 4-Amino-1,2,4-triazole–adipic acid (2:1); Crystal structure; Vibrational spectra; HF; B3LYP; MP2; Second harmonic generation

1. Introduction

The utilisation of the 1,2,4-triazole moiety as a part of ligand system in metal complexes has gained considerable attention in recent years [1–5]. The 1,2,4-triazole system is also of magnetochemical interest because it is able to act as a bridge between metal centres and mediate exchange coupling. Spin crossover compounds with iron(II) [2,6] can act as an example. The another application of triazole ligand lies in medical research – complex with Pt(II) [7] exhibit antitumor activity (human cancer) similar to cis-platin. Triazole derivatives are also used in the synthesis of antibiotics, fungicides, herbicides, plant growth hormone regulators [8], and potentially good corrosion inhibitors [9,10].

* Corresponding author. Tel.: +420 221 951 245; fax: +420 221 951 253.
E-mail address: irena.mat@atlas.cz (I. Matulková).

0022-2860/$ - see front matter © 2007 Elsevier B.V. All rights reserved.
doi:10.1016/j.molstruc.2007.03.007

Materials based on triazole compounds with dicarboxylic acids exhibit many important properties. The two carboxylic groups can form linear structures by hydrogen bonds [11] and these assemblies (for example with unsaturated dicarboxylic acid) can be used for charge transfer [12]. On the other hand, a molecule of saturated dicarboxylic acid can form an inert spacer between two triazole rings. Such materials can be used in optical research as molecular switches [13]. From the point of view of preparation of non-linear optical (NLO) crystals, these materials combine highly polarisable cations or molecules (i.e. carriers of non-linear properties) with hydrogen-bonding organic acids providing thermal and structural stability. This concept based on encapsulation of organic cations between chains or layers of organic or inorganic anions for building of acentric crystalline NLO materials was successfully applied for example in the case of 2-amino-5-nitropyridinium salts [14–16]. Another example of such a material based on the related 3-amino-1,2,4-triazole moiety consists in 3-amino-1,2,4-triazolinium(1+) hydrogen L-tartrate, which was studied [17] as a promising novel compound for second harmonic generation (SHG).

Hydrogen bonding is generally one of the most effective and popular tools for the design of crystal structures. The role of several types of hydrogen bonds in crystal engineering of NLO materials was widely discussed and explained [18–23]. Furthermore, hydrogen bonding in these compounds has a notable energetic contribution to the total lattice energy [24] and also contributes to the second-order NLO tensor coefficient (d_{ijk}) of the crystals [25,26].

Only a few papers concerning vibrational spectroscopic studies of triazoles and their compounds have been published yet [1,17,27,28]. Although detailed examination of vibrational spectra is important not only from the standpoint of characterization of promising new NLO materials but also with regard to the vibrational contribution to molecular hyperpolarizabilities in these materials [29–32].

This work is part of our project focused on preparation and study of new materials (based on hydrogen-bonded salts of organic cations) for SHG and deals with the systems capable of forming a variety of intermolecular hydrogen bonds based on 4-amino-1,2,4-triazole compounds with dicarboxylic acids. The crystal structures, vibrational spectra and optical properties of three new compounds: 4-amino-1,2,4-

Table 1
Basic crystallographic data, data collection and refinement parameters for **4-atox**, **4-atsuc** and **4-atadip**

Identification code	**4-atox**	**4-atsuc**	**4-atadip**
Empirical formula	$C_4H_6N_4O_4$	$C_6H_{10}N_4O_4$	$C_{10}H_{18}N_8O_4$
Formula weight	174.13	202.18	314.32
Temperature (K)	150(2)	150(2)	293(2)
a (Å)	3.7280(2)	11.8130(5)	6.3610(3)
b (Å)	18.349(1)	5.0690(3)	8.0580(2)
c (Å)	4.9680(4)	16.5280(5)	14.8750(5)
β (°)	101.134(5)	117.285(3)	104.072(2)
Volume (Å^3)	333.44(4)	879.58(7)	739.57(5)
Z	2	4	2
Calculated density (Mg/m^3)	1.734	1.527	1.411
Crystal system	Monoclinic	Monoclinic	Monoclinic
Space group	$P2_1$	$P2_1/c$	$P2_1/c$
Absorption coefficient (mm^{-1})	0.155	0.129	0.112
$F(000)$	180	424	332
Crystal size (mm)	$0.20 \times 0.18 \times 0.15$	$0.43 \times 0.40 \times 0.38$	$0.45 \times 0.40 \times 0.38$
Diffractometer and radiation		Nonius Kappa CCD, Mo $\lambda = 0.71073$ Å	
Scan technique		ω and ψ scans to fill the Ewald sphere	
Completeness to θ	27.46, 91.7%	27.48, 99.5%	27.47, 98.9%
Range of h, k and l	$-4 \to 4$, $-23 \to 23$, $-6 \to 6$	$-15 \to 15$, $-6 \to 4$, $-21 \to 20$	$-8 \to 8$, $-10 \to 10$, $-19 \to 19$
θ Range for data collection (°)	4.74–27.46	2.77–27.48	2.82–27.47
Reflection collected/unique (R_{int})	4240/1344 (0.0280)	7255/2011 (0.0260)	11290/1695 (0.0360)
No. of observed reflection	1328	1701	1695
Criterion for observed reflection		$I > 2\sigma(I)$	
Absorption correction		None	
Function minimized		$\Sigma w(F_o^2 - F_c^2)^2$	
Parameters refined	125	143	112
R, wR [$I > 2\sigma$(I)]	0.0284, 0.0749	0.0352, 0.0849	0.0487, 0.1258
R, wR (all data)	0.0289, 0.0753	0.0447, 0.0923	0.0640, 0.1380
Value of S	1.093	1.044	1.040
Max. and min. heights in final Δp map (eÅ^{-3})	0.207 and −0.158	0.252 and −0.249	0.423 and −0.397
Weighting scheme		$w = [\sigma^2(F_o^2) + (aP)^2 + bP]^{-1}$ $P = (F_0^2 + 2F_c^2)/3$	
	$a = 0.0432$	$a = 0.0432$	$a = 0.0936$
	$b = 0.0609$	$b = 0.0609$	$b = 0.2015$
Sources of atomic scattering factors		SHELXL97 [36]	
Programs used		SHELXL97 [36], PLATON [49], SIR97 [35]	

triazol-1-ium hydrogen oxalate (**4-atox**) salt and adducts of 4-amino-1,2,4-triazole with succinic acid (**4-atsuc**) and adipic acid (**4-atadip**) are presented and discussed.

2. Experimental

4-Amino-1,2,4-triazole (**4-at**) was prepared and purified by a slightly modified procedure described previously in the literature [33,34]: 6 ml (0.14 mol) of formic acid (90%, Lachema) and 11.5 ml (0.23 mol) of hydrazine monohydrate (99%, Fluka) were very carefully mixed under cooling in a water ice bath. The flask was equipped with a Liebig distillation condenser and heated (over 1 h) in a sand bath to a temperature of 200 ± 5 °C (measured in the sand bath). The excess of hydrazine and water was distilled off slowly. The distillation started when the temperature in the sand bath reached 195 °C and the mixture was heated for additional four hours after the end of the distillation. After standing overnight, the reaction mixture was heated to 200 °C under reduced pressure (water vacuum pump) for two hours to remove the residues of water and hydrazine. After cooling, the colourless melt solidified. The solid product was dissolved in 14.5 ml of ethanol and the same volume of diethyl ether and left to crystallise in a refrigerator. The reaction yield was 3.0 g (51%) of white needles, m.p. 354–355 K. The purity of the prepared compound was checked by ^{1}H and ^{13}C NMR spectra recorded on a 400 MHz Varian Unity spectrometer: ^{1}H NMR (DMSO, ref. DMSO δ 2.5 ppm) δ 6.2 (2H, d), 8.4 (2H, d). ^{13}C NMR (DMSO, ref. DMSO δ 39.5 ppm) δ 143.6 (s). The product was also characterised by its FTIR spectrum, which was compared to the literature [1,27].

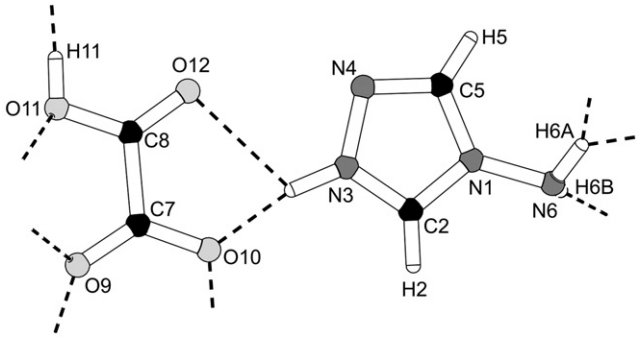

Fig. 1. Atom numbering of **4-atox**. Dashed lines indicate hydrogen bonds.

Crystals of **4-atox**, **4-atsuc** and **4-atadip** were prepared from equimolar mixtures of aqueous **4-at** solution with an aqueous solution of oxalic acid dihydrate (purum, Lachema) or methanolic solutions of succinic acid (p.a., Lachema) or adipic acid (purum, Lachema), respectively. The colourless solutions obtained were kept in a desiccator over sulphuric acid at room temperature. The colourless crystals prepared by slow spontaneous crystallisation were filtered off, washed with methanol and dried in a desiccator over

Table 2
Selected bond lengths (Å) and angles (°) for **4-atox**

Bond/angle	Value	Angle	Value
N(1)–C(2)	1.336(2)	C(2)–N(3)–N(4)	111.8(1)
N(1)–C(5)	1.362(2)	C(2)–N(3)–H(3)	123(2)
N(1)–N(6)	1.414(2)	N(4)–N(3)–H(3)	125(2)
C(2)–N(3)	1.311(2)	C(5)–N(4)–N(3)	103.8(2)
N(3)–N(4)	1.366(2)	N(4)–C(5)–N(1)	110.9(1)
N(4)–C(5)	1.309(2)	N(1)–N(6)–H(6A)	107(2)
C(7)–O(9)	1.239(2)	N(1)–N(6)–H(6B)	107(2)
C(7)–O(10)	1.266(2)	H(6A)–N(6)–H(6B)	115(2)
C(7)–C(8)	1.545(2)	O(9)–C(7)–O(10)	127.0(2)
C(8)–O(12)	1.211(2)	O(9)–C(7)–C(8)	118.8(1)
C(8)–O(11)	1.309(2)	O(10)–C(7)–C(8)	114.2(1)
C(2)–N(1)–C(5)	106.8(1)	O(12)–C(8)–O(11)	125.9(2)
C(2)–N(1)–N(6)	124.4(1)	O(12)–C(8)–C(7)	120.8(1)
C(5)–N(1)–N(6)	128.6(1)	O(11)–C(8)–C(7)	113.3(1)
N(3)–C(2)–N(1)	106.7(1)	C(8)–O(11)–H(11)	111(2)
Hydrogen bonds			

D–H···A	*d*(D–H)	*d*(H···A)	*d*(D···A)	<(DHA)
N(3)–H(3)···O(10)	1.01(3)	1.72(3)	2.711(2)	167(3)
N(3)–H(3)···O(12)	1.01(3)	2.40(3)	2.951(2)	113(2)
N(6)–H(6A)···O(9)	0.88(3)	2.21(3)	3.031(2)	154(2)
N(6)–H(6A)···O(11)^{i}	0.88(3)	2.35(2)	3.012(2)	132(2)
N(6)–H(6B)···O(9)^{ii}	0.82(2)	2.23(3)	2.921(2)	143(2)
O(11)–H(11)···O(10)^{iii}	0.84(3)	1.69(3)	2.531(2)	178(3)

Note. Symmetry transformations used to generate equivalent atoms: (i) $-x+1$, $y-1/2$, $-z+1$; (ii) $-x+1$, $y-1/2$, $-z+2$; (iii) $x-1$, y, $z-1$. *Abbreviations.* A, acceptor; D, donor.

Table 3
Selected bond lengths (A) and angles (°) for **4-atsuc**

Bond/angle	Value	Angle	Value
N(1)–N(6)	1.409(2)	C(2)–N(1)–N(6)	123.8(1)
N(1)–C(2)	1.347(2)	C(5)–N(1)–N(6)	129.9(1)
N(1)–C(5)	1.356(2)	C(5)–N(4)–N(3)	107.5(1)
N(4)–C(5)	1.309(2)	C(2)–N(3)–N(4)	107.0(1)
N(3)–N(4)	1.388(2)	N(4)–C(5)–N(1)	109.3(1)
C(2)–N(3)	1.307(2)	N(3)–C(2)–N(1)	110.0(1)
C(7)–O(12)	1.214(2)	O(12)–C(7)–O(11)	119.7(1)
C(7)–O(11)	1.326(2)	O(12)–C(7)–C(8)	123.2(1)
C(7)–C(8)	1.504(2)	O(11)–C(7)–C(8)	117.1(1)
C(8)–C(9)	1.522(2)	C(7)–C(8)–C(9)	112.3(1)
C(9)–C(10)	1.503(2)	C(10)–C(9)–C(8)	113.5(1)
C(10)–O(14)	1.217(2)	O(14)–C(10)–O(13)	123.1(1)
C(10)–O(13)	1.321(2)	O(14)–C(10)–C(9)	123.8(1)
N(1)–N(6)–H(6A)	110(1)	O(13)–C(10)–C(9)	113.0(1)
N(1)–N(6)–H(6B)	106(1)	C(7)–O(11)–H(11)	113(1)
H(6A)–N(6)–H(6B)	111(2)	C(10)–O(13)–H(13)	109(1)
C(2)–N(1)–C(5)	106.2(1)		
Hydrogen bonds			

D–H···A	*d*(D–H)	*d*(H···A)	*d*(D···A)	<(DHA)
N(6)–H(6A)···O(12)^{i}	0.90(2)	2.43(2)	2.848(2)	109(1)
N(6)–H(6A)···O(14)^{i}	0.90(2)	2.22(2)	3.053(2)	154(2)
N(6)–H(6B)···N(6)^{ii}	0.93(2)	2.28(2)	3.173(2)	161(2)
O(11)–H(11)···N(3)^{iii}	0.94(2)	1.76(2)	2.689(1)	169(2)
O(13)–H(13)···N(4)^{iv}	0.96(2)	1.71(2)	2.666(2)	171(2)

Note. Symmetry transformations used to generate equivalent atoms: (i) $-x+1$, $y-1/2$, $-z+3/2$; (ii) $-x+1$, $y+1/2$, $-z+3/2$; (iii) $-x+2$, $-y$, $-z+2$; (iv) x, $-y+1/2$, $z-1/2$. *Abbreviations.* A, acceptor; D, donor.

Table 4
Selected bond lengths (A) and angles (°) for **4-atadip**

Bond/angle	Value	Angle	Value
N(1)–C(2)	1.345(2)	N(3)–C(2)–N(1)	110.0(2)
N(1)–C(5)	1.347(2)	C(2)–N(3)–N(4)	107.6(2)
N(1)–N(6)	1.408(2)	C(5)–N(4)–N(3)	106.2(2)
C(2)–N(3)	1.302(2)	N(4)–C(5)–N(1)	110.7(2)
N(3)–N(4)	1.386(2)	N(1)–N(6)–H(6A)	104(2)
N(4)–C(5)	1.303(2)	N(1)–N(6)–H(6B)	111(2)
C(7)–C(7)^{i}	1.511(3)	H(6A)–N(6)–H(6B)	107(2)
C(7)–C(8)	1.512(3)	C(7)–C(7)–C(8)	113.2(2)
C(8)–C(9)	1.497(2)	C(9)–C(8)–C(7)	114.0(2)
C(9)–O(10)	1.208(2)	O(10)–C(9)–O(11)	121.6(2)
C(9)–O(11)	1.305(2)	O(10)–C(9)–C(8)	124.0(2)
C(2)–N(1)–C(5)	105.5(2)	O(11)–C(9)–C(8)	114.3(2)
C(2)–N(1)–N(6)	129.9(2)	C(9)–O(11)–H(11)	109(2)
C(5)–N(1)–N(6)	124.6(2)		

Hydrogen bonds

D–H···A	*d*(D–H)	*d*(H···A)	*d*(D···A)	<(DHA)
N(6)–H(6A)···O(10)^{ii}	0.91(2)	2.07(3)	2.940(2)	160(2)
N(6)–H(6B)···N(4)^{iii}	0.95(3)	2.40(3)	3.025(2)	123(2)
O(11)–H(11)···N(3)^{iii}	1.04(4)	1.63(4)	2.669(2)	175(3)

Note. Symmetry transformations used to generate equivalent atoms: (i) $-x+2,\ -y+1,\ -z+1$; (ii) $-x+1,\ y-1/2,\ -z+1/2$; (iii) $x-1,\ y,\ z$.
Abbreviations. A, acceptor; D, donor.

KOH (average dimensions of crystals were $0.5\times1.0\times6.0$, $0.5\times1.0\times1.5$ and $1.0\times1.5\times4.0$ mm for **4-atox**, **4-atsuc** and **4-atadip**, respectively).

Collection of X-ray data of **4-atox**, **4-atsuc** and **4-atadip** was performed on a Nonius Kappa CCD diffractometer (MoKα radiation, graphite monochromator). The temperature of the crystal was controlled by an Oxford Cryosystems liquid nitrogen Cryostream Cooler. The phase problem was solved by direct methods (SIR-92 [35]) and the non-hydrogen atoms were refined anisotropically, using the full-matrix least-squares procedure (SHELXL-97 [36]). Hydrogen atoms attached to carbon atoms were calculated in a geometrically idealized position with $C_{sp^3}-H = 0.97$ Å and $C_{sp^2}-H = 0.93$ Å, and constrained to ride on their parent atoms, with $U_{iso}(H) = 1.5\ U_{eq}(C)$. Hydrogens attached to oxygen and nitrogen atoms were localized on difference Fourier maps and refined isotropically. The basic crystallographic data, measurement and refinement details are summarized in Table 1.

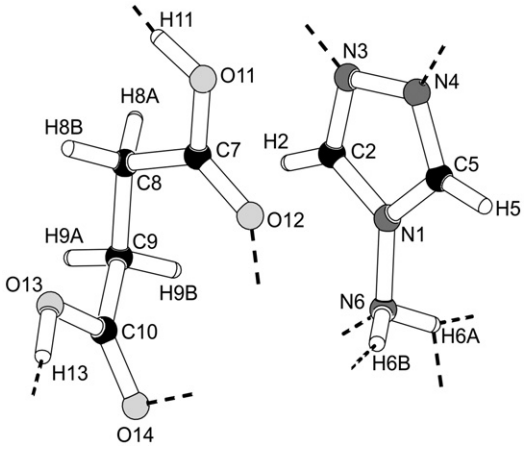

Fig. 3. Atom numbering of **4-atsuc**. Dashed lines indicate hydrogen bonds.

Crystallographic data for **4-atox**, **4-atsuc** and **4-atadip** have been deposited with the Cambridge Crystallographic Data Center as supplementary publications CCDC 252739, CCDC 252738 and CCDC 259835, respectively. Copies of the data can be obtained free of charge on application to CCDC, 12 Union Road, Cambridge CG21, EZ, UK (fax: +44 1223 336 033; e-mail: deposit@ccdc.cam.ac.uk).

The infrared spectra were recorded by nujol and fluorolube mull techniques on a Nicolet Magna 760 FTIR spectrometer with 2 cm^{-1} resolution (4 cm^{-1} resolution in FAR IR region) and Happ-Genzel apodization in the 85–4000 cm^{-1} region.

The Raman spectra of polycrystalline samples were recorded on a Nicolet Magna 760 FTIR spectrometer

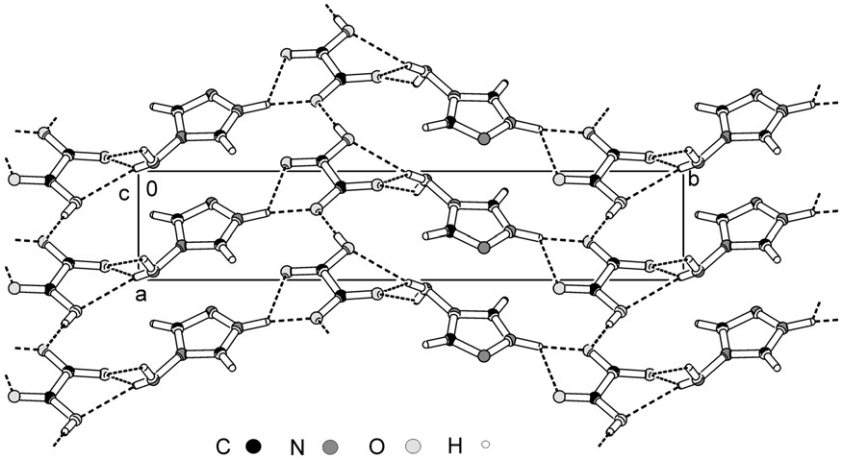

Fig. 2. Packing scheme of **4-atox** (projection to *xy* plane). Dashed lines indicate hydrogen bonds.

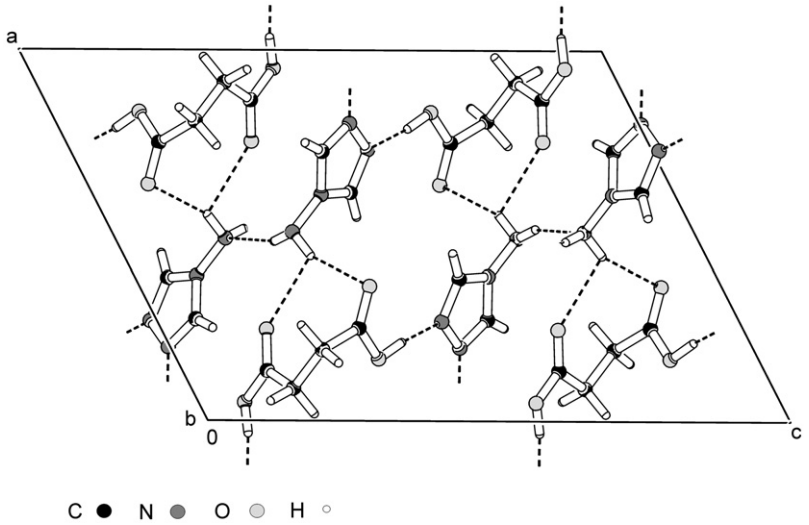

Fig. 4. Packing scheme of **4-atsuc** (projection to *xz* plane). Dashed lines indicate hydrogen bonds.

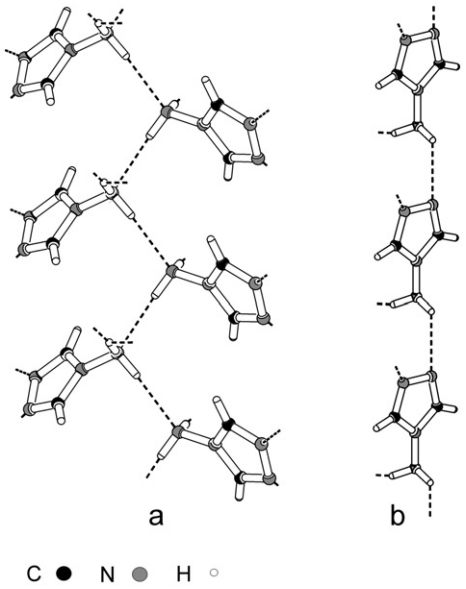

Fig. 5. The arrangement of **4-at** units: (a) Zig-zag arrangement in **4-atsuc** structure; (b) The arrangement in **4-atadip** structure. Dashed lines indicate hydrogen bonds.

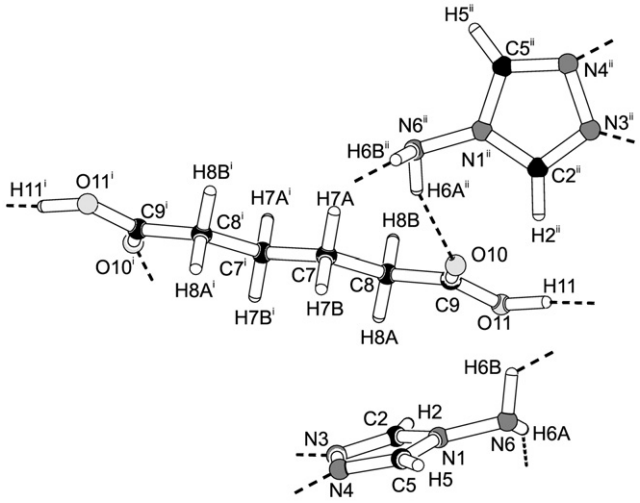

Fig. 6. Atom numbering in **4-atadip**. Dashed lines indicate hydrogen bonds.

equipped with Nicolet Nexus FT Raman module (2 cm^{-1} resolution, Happ-Genzel apodization, 1064 nm Nd:YVO_4 laser excitation, 450 mW power at the sample) in the 100–3700 cm^{-1} region.

The quantum chemical calculations were performed by applying closed-shell restricted Hartree–Fock (HF), Density Functional Theory (B3LYP) and Møller–Plesset perturbation (MP2) methods with the 6-31G and 6-311G basis sets. The calculations and visualisation of the results were carried out with the Gaussian 98W [37] and GaussView [38] program packages. The geometry optimisations, also yielding the molecular energies, were followed by frequency calculations together with IR and Raman intensities using the same basis set. The calculated geometry and frequencies scaled with precomputed vibrational scaling factors [39] were compared to the experimental values.

The UV–Vis–NIR spectrum of **4-atox** single crystal was recorded in the 190–1100 nm range using a Unicam UV 300 spectrometer.

The measurements of SHG at 800 nm were performed with 90 fs laser pulses generated at an 82 MHz repetition rate by a Ti:sapphire laser (Tsunami, Spectra Physics). For quantitative determination of the SHG efficiency, the intensity of the back-scattered laser light at 400 nm generated in the sample was measured by a grating spectrograph with diode array (InstaSpec II, Oriel) and the signal was compared with that generated in KDP (i.e. KH_2PO_4). The experiment was performed using a powdered sample

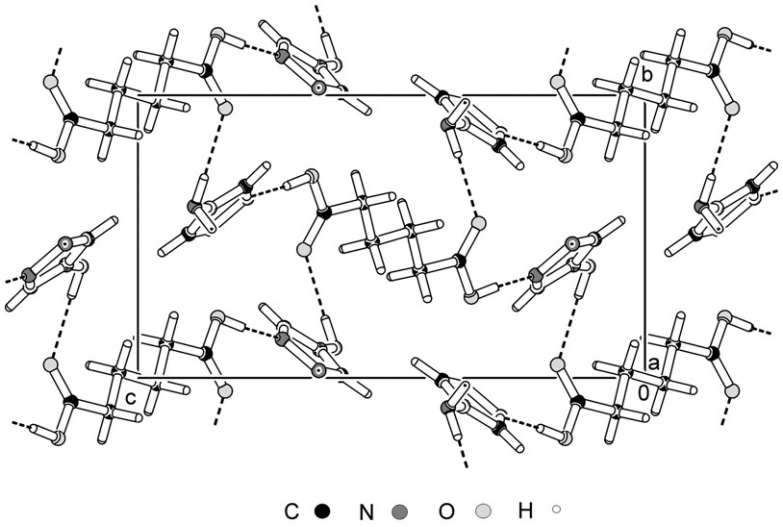

Fig. 7. Packing scheme of **4-atadip** (projection to *yz* plane). Dashed lines indicate hydrogen bonds.

(75–150 μm particle size) loaded into 5 mm glass cells using a vibrator and the measurements were repeated on different areas of the same sample (the results were averaged). This experimental procedure minimises the signal fluctuations induced by sample packing.

3. Results and discussion

3.1. Crystal structures

The crystals of **4-atox** belong in monoclinic system (space group $P2_1$). The bond lengths and angles including those of hydrogen bonds are listed in Table 2. The atom numbering is depicted in Fig. 1. The crystal structure consists of periodically alternating layers (parallel to *a* axis) formed by chains of hydrogen oxalate anions connected by O–H···O hydrogen bonds with lengths of 2.531(2) Å. The layers are interconnected by 4-amino-1,2,4-triazol-1-ium cations via N–H···O hydrogen bonds. These hydrogen bonds consist of a linear (two-center) H-bond (N6···O9^{i} distance equal to 2.921(2) Å) and two pairs of bifurcated (three-center) H-bonds, connecting the nitrogen atom N3 with oxygens O10 and O12 by the H3 atom (2.711(2) and 2.951(2) Å, respectively) and amine group nitrogen N6 with oxygens O9 and O11 by H6A atom (3.031(2) and 3.012(2) Å, respectively).

The formation of 4-amino-1,2,4-triazol-1-ium cation by protonation of the N3 atom results in minimal changes in the triazole ring geometry. Only slight shortening of the N1–C2 and N3–N4 distances compared to uncharged molecules were observed in the **4-atsuc** and **4-atadip** structures (see Tables 2–4). The cation rings are mutually oriented in parallel with no H-bonds interaction between them (see Fig. 2).

The lengths of the C–O bonds correspond with the existence of the hydrogen oxalate anion in the crystal structure. Elongation of the C7–O10 (1.266(2) Å) and C7–O9 (1.239(2) Å) bonds compared to the C8–O12 (1.211(2) Å) bond is in accordance with more intensive participation of the O10 and O9 atoms in the hydrogen bond system. Especially oxygen O10 participates in the two strongest hydrogen bonds of the O–H···O and N–H···O type.

The addition compound **4-atsuc** crystallizes in the monoclinic system with the space group $P2_1/c$. Bond lengths and angles including those of the hydrogen bonds are listed in Table 3 and the atom numbering is depicted in Fig. 3. The crystal structure is formed by zig-zag chains (parallel to *b* axis) of 4-amino-1,2,4-triazole molecules, connected by N–H···N hydrogen bonds, and isolated molecules of succinic acid, which interconnect these chains by strong O–H···N (2.666(2) and 2.689(1) Å) and medium to weak N–H···O hydrogen bonds (see Fig. 4).

The amine group of the base participates in the N–H···N hydrogen bonds (i.e. N6–H6B···N6^{ii} with the length of 3.173(2) Å) forming the chains (see Fig. 5a) and also in bifurcated bonds of N–H···O type connecting the N6 atom with oxygens O12 and O14 by H6A atom (2.848(2) and 3.053(2) Å, respectively).

The protonised carboxylic groups of succinic acid attain two different values for C–O (1.214(2) and 1.217(2) Å) and C–O(H) (1.326(2) and 1.321(2) Å) bond lengths.

The **4-atadip** addition compound, which crystallizes in a 2:1 (base to acid) ratio, belongs in the monoclinic system (space group $P2_1/c$). Bond lengths and angles including those of the hydrogen bonds are listed in Table 4. The atom numbering is depicted in Fig. 6. The crystal structure consists of pairs of parallel linear chains (mediated by N–H···N hydrogen bonds – see Fig. 5b) of 4-amino-1,2,4-triazole molecules that are interconnected by isolated adipic acid molecules via strong O–H···N and medium N–H···O hydrogen bonds (see Fig. 7) with

Table 5
Comparison of the results of X-ray structure determination and computational geometry optimisation for 4-amino-1,2,4-triazole molecule (**4-at**)

X-ray structure determination						Geometry optimisation					
						B3LYP/6-311G		HF/6-311G		MP2/6-311G	
Bond	**4-atsuc** (Å)	**4-atadip** (Å)	Angle	**4-atsuc** (°)	**4-atadip** (°)	Bond (Å)	Angle (°)	Bond (Å)	Angle (°)	Bond (Å)	Angle (°)
N(1)–C(2)	1.347(2)	1.345(2)	N(1)–N(6)–H(6A)	109.8(1)	104(2)	1.370	113.67	1.360	113.84	1.380	112.23
N(1)–C(5)	1.356(2)	1.347(2)	N(1)–N(6)–H(6B)	106.2(1)	111(2)	1.380	113.67	1.360	113.85	1.380	112.19
N(1)–N(6)	1.409(2)	1.408(2)	N(3)–C(2)–N(1)	110.0(1)	110.0(2)	1.398	110.49	1.379	109.85	1.410	110.49
N(3)–N(4)	1.388(2)	1.386(2)	N(4)–C(5)–N(1)	109.3(1)	110.7(2)	1.430	110.09	1.390	109.67	1.450	110.32
N(4)–C(5)	1.310(2)	1.303(2)	C(2)–N(1)–C(5)	106.2(1)	106(2)	1.320	105.75	1.290	105.37	1.340	106.24
N(6)–H(6A)	0.90(2)	0.91(2)	C(2)–N(1)–N(6)	123.8(1)	129.9(2)	1.000	124.81	0.990	125.18	1.010	124.20
N(6)–H(6B)	0.930(2)	0.95(3)	C(2)–N(3)–N(4)	107.0(1)	107.6(2)	1.000	106.72	0.990	107.34	1.010	106.41
C(2)–N(3)	1.307(2)	1.302(2)	C(5)–N(1)–N(6)	129.9(1)	124.6(2)	1.320	129.43	1.290	129.44	1.340	129.55
			C(5)–N(4)–N(3)	107.5(1)	106.2(2)		106.85		107.68		106.43
			H(6A)–N(6)–H(6B)	111.3(2)	107(2)		115.40		115.57		114.55

lengths of 2.669(2) and 2.940(2) Å, respectively. Neighbouring chains, which are parallel to the *a* axis, do not exhibit any H-bond contact between each other. The N–H···N hydrogen bonds with a length of 3.025(2) Å connect nitrogen atom N6 of amine group with triazole ring atom N4. Different crystal packing (compared to **4-atsuc**) is mainly induced by the enhanced steric requirements of adipic acid.

As in the case of **4-atsuc**, the protonised carboxylic groups of adipic acid exhibit two different values for the C–O (1.208(2) Å) and C–O(H) (1.305(2) Å) bond lengths.

3.2. Geometric optimisation and calculation of vibrational frequencies

In order to assign the vibrational manifestations of 4-amino-1,2,4-triazole and 4-amino-1,2,4-triazol-1-ium species, computational geometry optimisation followed by vibrational frequencies calculation were performed. The selection of functionals (HF, MP2, B3LYP) and basis sets (6-31G and 6-311G) in principle results from the previous paper [27] dealing with triazoles.

The results obtained from geometry calculations are compared with the X-ray structure determination in Tables 5 and 6. According to this comparison, the best results were obtained for the HF method with the 6-311G basis set for both calculated species. In the HF method, the value of the bond lengths fluctuate around the values obtained from the crystal data. Application of the MP2 and B3LYP methods leads to systematic overestimation of the bond lengths except for the value for the N1–N6 bond in the case of the B3LYP methods. The values of the inter-atomic angles fluctuate slightly around the values obtained in the crystal structure determinations.

Tables 7 and 8 contain the calculated and experimental values of the fundamental frequencies of the 4-amino-1,2,4-triazole molecule and the 4-amino-1,2,4-triazol-1-ium cation, respectively. The intensities of the calculated IR and Raman bands are presented on a relative scale from 0 to 100. The proposed assignment of the vibrational bands is based on visualisation of the atom motions in the GaussView [38] program. The best match with experimental records was again observed for the HF/6-311G method. The largest differences between the calculated and recorded peak positions were observed for the stretching N–H vibrations because the formation of hydrogen bonds was not reflected in the calculations.

3.3. Vibrational spectra

The FTIR and FT Raman spectra of **4-atox, 4-atsuc** and **4-atadip** recorded at room temperature are depicted in Figs. 8–10, respectively. The assignment of the observed bands is based on ab initio calculations (HF/6-311G) of **4-at** and **4-at(1+)** vibrational spectra and previous papers concerning 4-amino-1,2,4-triazole [1] and carboxylic acids [40–43].

Table 6
Comparison of the results of X-ray structure determination and computational geometry optimisation for 4-amino-l,2,4-triazol-l-ium cation (**4-at(l+)**)

X-ray structure determination for **4-atox**				Geometry optimisation					
				B3LYP/6-311G		HF/6-311G		MP2/6-311G	
Bond	(Å)	Angle	(°)	Bond (Å)	Angle (°)	Bond (Å)	Angle (°)	Bond (Å)	Angle (°)
N(1)–C(2)	1.336(2)	N(1)–N(6)–H(6A)	106(2)	1.355	115.00	1.330	114.42	1.360	112.94
N(1)–C(5)	1.362(2)	N(1)–N(6)–H(6B)	107(2)	1.390	115.00	1.380	114.39	1.390	112.95
N(1)–N(6)	1.414(2)	N(3)–C(2)–N(1)	106.7(1)	1.390	105.84	1.370	106.26	1.400	105.59
N(3)–N(4)	1.366(2)	N(4)–N(3)–H(3)	125(2)	1.390	118.69	1.370	119.32	1.400	118.53
N(3)–H(3)	1.01(3)	N(4)–C(5)–N(1)	110.9(1)	1.000	110.70	0.990	109.98	1.010	110.35
N(4)–C(5)	1.309(2)	C(2)–N(1)–C(5)	106.8(1)	1.310	107.08	1.280	107.26	1.340	108.04
N(6)–H(6A)	0.88(3)	C(2)–N(1)–N(6)	124.4(1)	1.000	123.21	0.990	123.42	1.010	122.06
N(6)–H(6B)	0.82(2)	C(2)–N(3)–N(4)	112(1)	1.000	112.45	0.990	111.71	1.010	112.66
C(2)–N(3)	1.311(2)	C(2)–N(3)–H(3)	123(2)	1.320	128.84	1.300	128.94	1.340	128.79
		C(5)–N(1)–N(6)	128.6(1)		129.69		129.32		129.90
		C(5)–N(4)–N(3)	103.8(2)		103.87		104.75		103.33
		H(6A)–N(6)–H(6B)	115(2)		118.23		117.56		116.56

*3.3.1. Vibrational spectra of **4-atox***

The strong bands in the 3300–2200 cm^{-1} region in the IR spectrum correspond to the stretching vibrations of the N–H groups connected to the N–H···O hydrogen bonds with lengths of 3.031–2.711 Å. The band attributed to the out-of-plane bending mode γN–H(···O) is located at 972 cm^{-1} in the infrared spectrum. The broad, medium intensity bands in the 2100–1850 cm^{-1} region in the IR spectrum (assigned to the O–H stretching vibrations) reflect the presence of the short O–H···O hydrogen bond with a length of 2.531 Å. The recorded positions of the bands of the N–H and O–H stretching vibrations are in agreement with the correlation curves [44,45] for the N–H···O and O–H···O hydrogen bonds, which were found in **4-atox** crystal structure.

The band of the stretching C=O vibration, which is characteristic for the presence of the protonised carboxylic group in the crystal structure, were recorded at 1717 cm^{-1} (IR spectrum) and 1723 cm^{-1} (Raman spectrum). The strong to medium-intensity bands of the antisymmetric (overlapping with triazole vibrations) and symmetric stretching vibrations of carboxylate COO^- group were observed in the IR spectrum at 1590 and 1428 cm^{-1}, respectively. Other significant manifestations of the hydrogen oxalate anion are the strong IR-active bands of the mixed δCOH, νC–O and νCC vibrations at 1266 and 1232 cm^{-1} or the bands of the mixed νCC, δCOO and δCOH vibrations at 913, 901 cm^{-1} (IR) and 890 cm^{-1} (Raman). The bands of the δCOO vibrations at 713 cm^{-1} (IR) or 710 cm^{-1} (Raman) and ωCOO vibrations at 486 cm^{-1} (IR) or 491 cm^{-1} (Raman) are also characteristic.

The bands assigned to the triazole C–H group stretching vibrations were observed at 3148 and 3112 cm^{-1} in the Raman spectrum and at 3156 cm^{-1} in the IR spectrum. The strong band at 1656 cm^{-1} recorded in the IR spectrum is attributed to the deformation vibration of the NH_2 group attached to the triazole ring. The most characteristic band related to the existence of 4-amino-1,2,4-triazolinium(1+) cation in the **4-atox** structure is the very strong Raman band of mixed νring, νN–NH_2, δNH and δCH vibrations at 1405 cm^{-1} (1408 cm^{-1} in the IR spectrum). The medium intense bands located in the 1075–1030 cm^{-1} region, which were assigned to the mixed νring, δCH and δNH vibrations, are similarly significant. For the assignment of the rest of the **4-at** (**1+**) vibrational bands, see Table 9.

*3.3.2. Vibrational spectra of **4-atsuc** and **4-atadip***

The structured, strong to medium-intensity bands in the IR spectra and weak bands in the Raman spectra in the 3400–2900 cm^{-1} region of the both compounds are associated (according to [44,45]) with the stretching vibrations of the N–H bonds, which participate in the hydrogen bonds of N–H···N (with the lengths of 3.025 and 3.173 Å) or N–H···O (with lengths of 3.053 and 2.848 Å) types.

The manifestations of strong O–H···N hydrogen bonds with the lengths of 2.666 and 2.689 Å (**4-atsuc**) or 2.669 Å (**4-atadip**) are very interesting. The corresponding IR bands (according to H-bonds lengths) of the stretching O–H vibrations are located in the 2900–2200 cm^{-1} region. In any case, broad, weak to medium-intensity bands with maxima at 1865 cm^{-1} (**4-atsuc**) and 1930 cm^{-1} (**4-atadip**) can be interpreted as the result of Fermi interaction of O–H stretching vibration with the overtones of bending modes. For example, similar bands were also observed in the IR spectra of the complexes formed by pyrazoles [46]. Bands that can be assigned to out-of-plane γO–H(···N) bending modes were recorded in the 850–1010 cm^{-1} region in the IR spectra of both addition compounds.

The stretching modes of the CH_2 groups of dicarboxylic acids were recorded in the 2950–2860 cm^{-1} region. The more complicated structure of these bands observed in the case of **4-atadip** is in accordance with the higher number of CH_2 groups in the molecule of adipic acid. The bands of characteristic νC=O stretching modes of carboxylic groups, which are very intensive in the IR spectra, are

Table 7
Calculated (scaled) and measured fundamental frequencies (cm^{-1}) of **4-at** molecule

B3LYP				MP2				HF				Measured 4-amino-1,2,4-triazole		
6-31G S.F.[a] 0.962	IR/ Raman intensities	6-311G S.F.[a] 0.966	IR/ Raman intensities	6-31G S.F.[a] 0.957	IR/ Raman intensities	6-311G S.F.[a] 0.950	IR/ Raman intensities	6-31G S.F.[a] 0.903	IR/ Raman intensities	6-311G S.F.[a] 0.904	IR/ Raman intensities	Assignment	IR	Raman
230	0/1	232	0/0	220	0/1	220	0/1	**241**	0/1	235	0/1	γC–N–NH_2		258 w
305	15/4	301	20/3	291	38/5	286	31/4	352	14/5	343	23/3	τNH_2	353 wb	394 w
386	3/2	384	3/2	370	6/6	365	5/2	397	2/2	393	4/1	δC–N–NH_2	417 m	405 w
491	100/3	561	100/2	470	26/0	533	24/0	564	100/4	635	30/1	γrg		
615	14/0	617	19/0	588	51/7	587	2/0	643	22/1	640	100/1	ωNH_2, νN–NH_2, δrg	620 s	629 w
656	0/0	658	0/0	628	1/0	625	25/7	688	0/1	687	0/1	γrg, τNH_2		
680	3/6	685	11/7	651	100/5	651	1/1	699	6/7	709	37/7	ωNH_2, δrg	680 m	679 vs
798	2/1	789	2/1	764	6/2	750	21/0	890	1/1	864	1/0	γCH	852 s	851 w
826	9/0	819	13/0	791	14/5	778	100/4	919	7/1	892	12/1	γCH	889 s	
													880 s	880 w
830	0/7	845	1/8	794	22/1	803	3/6	922	1/10	949	1/3	δrg, νrg, δCH	939 s	940 w
908	0/2	911	1/2	869	2/3	865	2/3	949	0/3	955	2/11	νrg, δCH	957 s	961 s
1029	14/4	1027	20/4	985	19/4	976	20/5	1045	19/5	1039	32/5	νrg, δCH	1070 s	1074 s
1157	7/4	1155	8/6	1107	26/6	1098	19/10	1205	3/7	1198	1/7	δCH	1186 s	1189 s
1172	0/5	1169	1/4	1122	1/4	1110	1/3	1210	5/5	1209	9/6	δCH, νN–NH_2 νrg	1205 s	1208 s
1243	0/1	1243	0/2	1189	7/2	1181	5/3	1276	0/3	1280	0/3	νrg, δrg, δCH, δNH_2	1292 m	
													1321 s	1321 w
1244	0/2	1265	0/3	1191	0/3	1202	0/4	1280	0/2	1298	1/4	ρNH_2	1346 m	1345 m
1348	0/12	1342	1/14	1290	0/8	1275	0/8	1413	0/16	1410	7/21	νrg, νN–NH_2, δCH	1382 m	1378 s
1406	2/1	1400	3/1	1346	1/4	1330	0/3	1493	5/0	1479	5/0	νrg, δCH	1452 s	1449 w
1452	6/4	1455	8/4	1389	16/2	1382	13/2	1530	16/9	1530	27/8	νrg, νN–NH_2, δCH, δNH_2	1518 s	1517 m
1652	7/12	1671	11/11	1581	17/12	1587	17/11	1679	10/9	1694	16/9	δNH_2	1625 m	1629 w
3196	0/40	3170	0/41	3058	0/48	3012	0/50	3162	0/44	3127	0/44	νCH	3101 m	3108 s
3214	0/67	3190	1/69	3076	1/73	3030	0/76	3181	0/75	3147	1/75	νCH	3122 m	3124 s
3426	2/100	3404	1/100	3279	5/100	3233	2/100	3432	4/100	3401	3/100	νNH_2	3200–3330	
3558	6/47	3532	6/45	3405	13/48	3355	9/46	3563	11/49	3524	10/49	νNH_2		

Note. Abbreviations and symbols: ν, stretching; δ, deformation or in-plane bending; γ, out-of-plane bending; ω, wagging; τ, torsion; ρ, rocking; rg, ring.

[a] Precomputed vibrational scaling factor [39].

Table 8
Calculated (scaled) and measured fundamental frequencies (cm^{-1}) of **4-at(l+)** cation

B3LYP				MP2				HF				Measured 4-amino-1,2.4-triazol-1-ium chloride		
6-31G S.F.[a] 0.962	IR/ Raman intensities	6-311G S.F.[a] 0.966	IR/ Raman intensities	6-31G S.F.[a] 0.957	IR/ Raman intensities	6-311G S.F.[a] 0.950	IR/ Raman intensities	6-31G S.F.[a] 0.903	IR/ Raman intensities	6-311G S.F.[a] 0.904	IR/ Raman intensities	Assignment	IR	Raman
247	13/3	251	10/1	236	3/1	239	2/1	273	1/1	264	1/1	γC–N–NH_2	290 m	283 w
273	2/2	273	6/2	261	19/5	260	22/3	351	11/4	345	17/53	τNH_2		334 w
374	70/1	389	11/1	358	4/2	370	4/2	402	4/1	400	4/12	δC–N–NH_2	428 m 443 m	412 m
430	89/4	465	100/3	412	76/6	441	63/5	519	100/5	574	100/4	ωNH_2	569 w	575 w
627	17/0	629	13/0	600	16/0	597	19/0	648	12/1	639	18/0	γrg, γCH	624 s	627 w
652	7/0	652	5/0	624	4/0	619	0/0	669	15/1	665	12/1	γrg, γCH, γNH	665 m	663 w
695	3/7	695	5/8	665	38/6	661	48/6	705	7/7	708	17/8	ωNH_2, νrg, δCH	678 m	680 s
790	71/1	789	59/0	756	52/1	750	61/0	843	53/1	812	64/0	γNH, γCH	838 m	
863	8/1	855	6/0	826	27/1	813	22/0	924	6/4	915	4/1	γCH	883 m	890 w
894	7/3	900	0/0	855	1/0	855	1/0	941	3/1	936	7/3	νrg, δrg, δNH, δCH	932 s	933 w
903	0/0	903	6/3	864	3/4	858	5/3	990	4/5	996	0/0	γCH, γNH, δrg		
958	2/4	966	3/5	917	0/5	918	1/7	1027	0/0	1004	12/6	νrg, δCH	1027 s	1033 s
1027	7/9	1025	8/10	983	7/9	974	7/12	1045	7/9	1041	7/11	νrg, δCH, δNH	1078 m	1077 s
1133	4/5	1134	4/5	1084	6/7	1077	6/8	1159	3/4	1157	3/4	νrg, γCH, δNH	1165 w	1157 m
1187	2/2	1187	2/3	1136	3/3	1128	4/5	1216	2/3	1217	3/4	γCH, νrg	1206 m	1209 m
1243	0/1	1246	2/7	1190	4/3	1184	4/3	1280	1/13	1281	2/14	νrg, δrg, δCH, δNH	1311 m	1314 m
1247	2/6	1265	0/2	1193	0/2	1202	0/3	1288	0/2	1302	0/3	ρNH_2	1327 m	1334 m
1339	4/8	1340	3/8	1281	4/21	1273	3/23	1372	3/5	1372	4/5	νrg, νN–NH_2, δNH, δCH	1360 m	1361 m
1386	3/20	1380	2/21	1327	5/5	1311	5/4	1464	1/22	1456	3/27	νrg, νN–NH_2, δNH, δCH	1408 m	1411 vs
1471	8/5	1471	8/5	1408	15/3	1397	17/4	1527	19/8	1518	2/7	νrg, δNH, δCH, νN–NH_2	1521 m	1523 w
1513	13/2	1515	9/2	1448	4/4	1439	3/3	1584	8/4	1581	2/4	νrg, δNH_2, δNH, δCH	1556 w	1553 w
1645	17/7	1661	16/7	1574	17/8	1578	20/8	1677	17/8	1688	22/8	δNH_2	1637 m	1644 w
3212	33/20	3186	23/23	3074	31/17	3027	29/22	3163	19/34	3131	20/34	νCH		3114 sh
3220	6/79	3195	5/76	3081	4/90	3035	5/85	3177	6/75	3145	6/72	νCH	3130 s	3134 m
3446	35/100	3421	22/100	3298	26/100	3250	23/100	3422	22/100	3398	19/99	νNH_2	3195 s	3210 w
3511	100/64	3519	79/64	3360	100/63	3343	100/65	3509	82/62	3518	94/65	νNH_2		
3591	36/43	3564	23/42	3437	29/46	3386	27/43	3567	29/46	3536	26/45	νNH		

[a] Precomputed vibrational scaling factor [39].

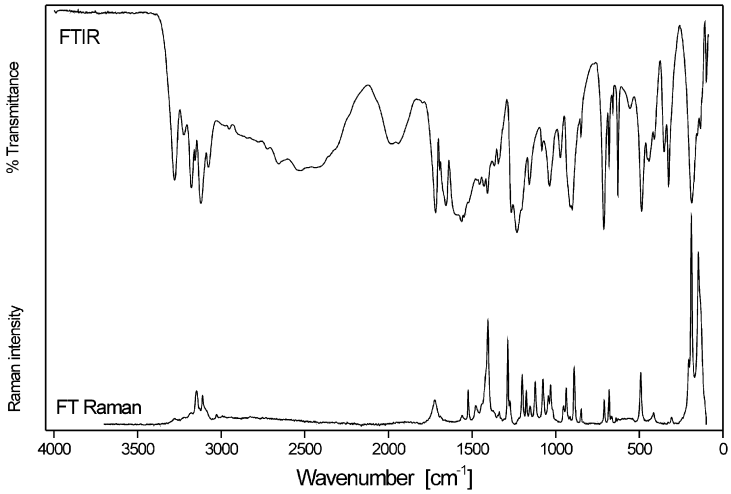

Fig. 8. FTIR (compiled from nujol and fluorolube mulls) and FT Raman spectra of **4-atox**.

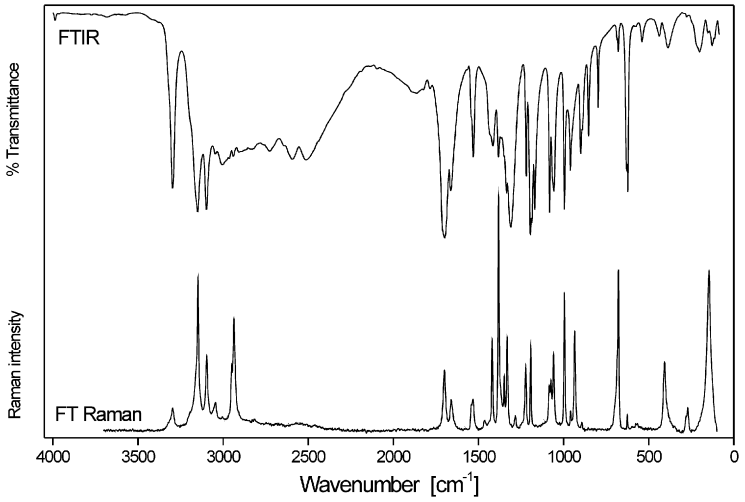

Fig. 9. FTIR (compiled from nujol and fluorolube mulls) and FT Raman spectra of **4-atsuc**.

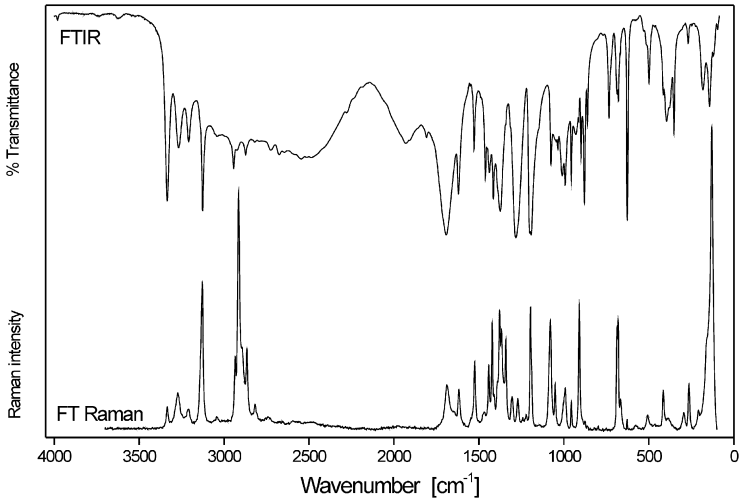

Fig. 10. FTIR (compiled from nujol and fluorolube mulls) and FT Raman spectra of **4-atadip**.

Table 9
FTIR and FT Raman spectra of **4-atox**

IR (cm^{-1})	Raman (cm^{-1})	Assignment
3280 m	3278 w	νN–H(···O)
3224 w	3224 w	
3177 m	3181 w	
3156 m	3148 m	νCH
3122 s		νN–H(···O)
	3112 m	νCH
3077 m		νN–H(···O)
	3027 w	
	2993 w	
	2938 w	
2660 mb	2828 w	
2525 mb		
2430 mb		
1982 mb		νO–H(···O)
1942 mb		
1717 s	1723 m	νC=O
1694 m	1690 w	?
1656 s		δNH_2
1590 sb		$\nu_{as}COO^-$
1565 s		νrg, δNH_2, δNH, δCH
1561 s	1560 w	
1550 s		
1521 s	1523 m	νrg, δNH_2, δNH, δCH, νN–NH_2
1470 m	1478 w	νC–O, δCOH, νCC
1455 m	1441 w	
1428 m		$\nu_s COO^-$
1408 s	1405 vs	νrg, νN–NH_2, δNH, δCH
1368 m	1380 w	
1343 m		ρNH_2
1336 sh	1337 w	
1316 sh	1308 w	νrg, δrg, δCH, δNH
	1287 s	δCOH, νC–O
1266 s	1274 w	δCOH, νC–O, νCC
1232 s		δCOH, νC–O, νCC
1204 sh	1200 s	γCH, νrg
	1175 m	δCOH, νC–O, νCC
1159 m	1154 w	νrg, γCH, δNH
	1123 m	?
1083 m	1076 m	νrg, δCH, δNH
1037 m	1044 m	νrg, δCH
	1031 m	
972 m		γN–H(···O)
	954 w	?
930 sh	937 m	νrg, δrg, δNH, δCH
913 s		νCC, δCOO, δCOH
901 s	890 s	νCC, δCOO, δCOH, γCH
850 w	848 w	γNH, γCH
713 s	710 m	δCOO
681 m	681 m	ωNH_2, νrg, δCH
	669 w	γrg, γCH, γNH
658 w	663 w	
	639 w	?
628 s	627 w	γrg, γCH
556 w	560 w	ωNH_2
486 s	491 s	ωCOO
451 m		δC–N–NH_2
442 m		
410 w	415 w	δCOO
351 m		τNH_2
325 m		ρCOO
	307 w	γC–N–NH_2
	205 s	External modes
187 s	188 vs	
152 w	147 vs	
134 w		
99 w		

Note. Abbreviations and symbols: vs, very strong; s, strong; m, medium; w, weak; b, broad; sh, shoulder; rg, ring; ν, stretching; δ, deformation or in-plane bending; γ, out-of-plane bending; ρ, rocking; ω, wagging; twi, twisting; τ, torsion; subscript s, symmetric; subscript as, antisymmetric.

Table 10
FTIR and FT Raman spectra of **4-atsuc**

IR (cm^{-1})	Raman (cm^{-1})	Assignment
3298 m	3297 w	νN–H(···O), νN–H(···N)
3149 s	3147 vs	νCH
3099 s	3096 m	
3047 m	3045 w	νN–H(···O)
3007 mb	3004 w	
	2950 m	νCH_2
2940 m	2936 s	
2890 mb		νO–H(···N)
2830 mb	2817 w	
2730 mb		
2595 mb	2570 w	
2515 mb		
1865 wb		
1786 w		?
1699 s	1699 m	νC=O
1664 m	1661 w	δNH_2
1541 sh	1541 w	νrg, νN–NH_2, δCH, δNH_2
1531 m	1532 w	
	1463 w	νrg, δCH
1430 sh		δCH_2
1416 m	1419 m	
1383 m	1382 vs	νrg, νN–NH_2, δCH
1349 sh	1349 m	ρNH_2
1335 m	1331 m	νrg, δrg, δCH, δNH_2
1310 s		νC–O, ωCH_2, νCC, ρCOO
	1284 w	twi CH_2
1219 m	1223 m	δCH, νN–NH_2, νrg
1194 s	1193 m	δCOH, ωCH_2, δCH
1186 s		
1169 s		twi CH_2
1082 s	1085 w	νCC, δCCC
	1075 m	νrg, δCH
1057 m	1059 m	
995 m	996 s	
961 m	959 w	
	935 s	νCC, δCCC
899 m		γCH, νCC, νC–O
890 sh	893 w	
853 m		γCH, γO–H(···N)
797 w		ρCH_2, γCOO, twi CH_2
679 w	678 vs	ωNH_2, δrg
628 m		ρCOO, νC–O
623 s	626 w	ωNH_2, νN–NH_2, δrg
540 w	565 w	γCOO, ρCH_2, γCOH
437 w		?
	407 m	δC–N–NH_2
387 w		τNH_2, δC–O, νCC
277 w	270 w	γC–N–NH_2
202 w		δCCC, δC–O
150 w	146 s	twi CC, ρCH_2
127 w		External modes
113 w		
81 w		

located at 1699 cm^{-1} (**4-atsuc**) and 1693 cm^{-1} (**4-atadip**). If the positions of this vibration recorded in the IR spectra of all three compounds (1717 cm^{-1} in **4-atox**) are compared, a red shift with increasing chain length of the acid is observed. This trend is in agreement with earlier studies [40] concerning saturated n-aliphatic acids. Other significant bands connected with the presence of carboxylic groups are the strong bands in the IR spectra at 1310, 1194 and 1186 cm^{-1} (**4-atsuc**) or 1283, 1202 and 1193 cm^{-1} (**4-atadip**), which are associated especially with the νC–O, δCOH and ωCH_2 mixed vibrations. The stretching νCC vibrations of the skeleton of dicarboxylic acids are the predominant vibrational motion linked with the strong Raman bands recorded at 935 and 910 cm^{-1} in the spectra of **4-atsuc** and **4-atadip**, respectively. For the assignment of the rest of the vibrational manifestations of succinic and adipic acids in studied addition compounds, see Tables 10 and 11, respectively.

The bands assigned to the stretching C–H vibrations of triazole ring were observed in the 3180–3070 cm^{-1} region. Contrary to our expectations and the results of vibrational spectra calculations, only one band of the νCH vibration was recorded in the case of **4-atadip**. This observation is even more interesting in regard of the presence of two 4-amino-1,2,4-triazole molecules in the asymmetric unit of **4-atadip**. Medium intensity bands corresponding to the deformation vibration of the NH_2 group, attached to the triazole ring, were observed at approx. 1660 and 1620 cm^{-1} in the spectra of **4-atsuc** and **4-atadip**, respectively. The blue shift of this vibration in the case of **4-atsuc** compared to **4-atadip** is connected with more intensive participation of the NH_2 group in the system of N–H···O and N–H···N hydrogen bonds in the crystal structure of **4-atsuc**. The most characteristic bands of the 4-amino-1,2,4-triazole molecule are located at approx. 1530, 1385, 1075, 680 and 625 cm^{-1} in the spectra of both addition compounds. For their particular assignment see Tables 10 and 11.

3.4. Second harmonic generation

Non-centrosymmetric crystals of **4-atox** (monoclinic space group $P2_1$) are optically transparent down to 300 nm (see Fig. 11) and thermally stable up to the melting point at 454 K. Quantitative measurements of the SHG efficiency were carried out at 800 nm by the modified powder technique developed by Kurtz and Perry [47]. The relative efficiency of powdered **4-atox** was observed as equal to 38% compared to KDP. The observed intensity dependence of SHG is depicted on Fig. 12.

Discussed crystals of **4-atox** can serve as another example of NLO material based on encapsulation of highly polarisable organic cations carrying NLO properties between the layers of hydrogen bonding organic anions.

Table 11
FTIR and FT Raman spectra of **4-atadip**

IR (cm^{-1})	Raman (cm^{-1})	Assignment
3335 s	3335 w	νN–H(···O), νN–H(···N)
3268 m	3273 w	
3209 m	3208 w	
3127 s	3129 s	νCH
3043 m	3045 w	νN–H(···O), νO–H(···N)
2945 m	2935 m	νCH_2
2925 m	2915 vs	
2873 m	2867 m	
2820 m	2818 w	νO–H(···N)
2792 m		
2725 m	2740 w	
2676 m		
2644 m	2660 w	
2545 mb	2570 w	
2513 m	2500 w	
2490 m		
1930 mb		
1809 m		?
1693 s	1689 m	νC=O
1621 m	1618 m	δNH_2
1529 m	1525 m	νrg, νN–NH_2, δCH, δNH_2
1463 m	1470 w	δCH_2, νrg, δCH
1439 m	1443 m	
	1422 s	ωCH_2
1416 s	1411 w	
1390 sh	1392 m	νrg, νN–NH_2, δCH
1375 s	1379 s	
	1367 s	
1343 sh	1342 m	ρNH_2
1314 sh	1305 w	twi CH_2
1283 s	1272 w	ωCH_2, δCOH, νC–O
	1242 w	ωCH_2, δCOH, νC–O
	1223 w	twi CH_2, ρCH_2
1202 s		ωCH_2, δCOH, νC–O, δCH,
1193 s	1197 s	νN–NH_2, νrg
1077 m	1080 s	νrg, δCH, νCC, δCCC
1036 m	1052 m	νCC
1010 m		γO–H(···N)
992 m	992 m	
957 m	957 w	νrg, δCH
930 m		δrg, νrg, δCH, ρCH_2, γCOO
913 w	910 s	νCC, νC–O
899 m		γCH
880 s		
862 w	876 w	
734 w		ρCH_2
687 w	687 s	ωNH_2, δrg, ρCOO, δCCC
679 w	681 s	ωNH_2, δrg
668 w	667 w	ρCOO
627 s	628 w	ωNH_2, νN–NH_2, δrg
499 w	507 w	δC–O , νCC, δCCC
415 w	415 w	δC–N–NH_2
396 m	393 w	τNH_2
378 w	385 w	
353 m		
	295 w	?
269 w	264 m	γC–N–NH_2
	209 w	External modes
182 w		
143 w	130 vs	
121 w		

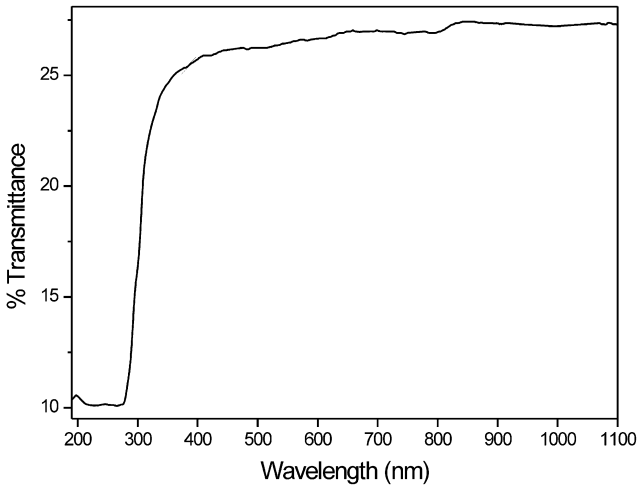

Fig. 11. UV–Vis–NIR spectrum of **4-atox** single crystal plate.

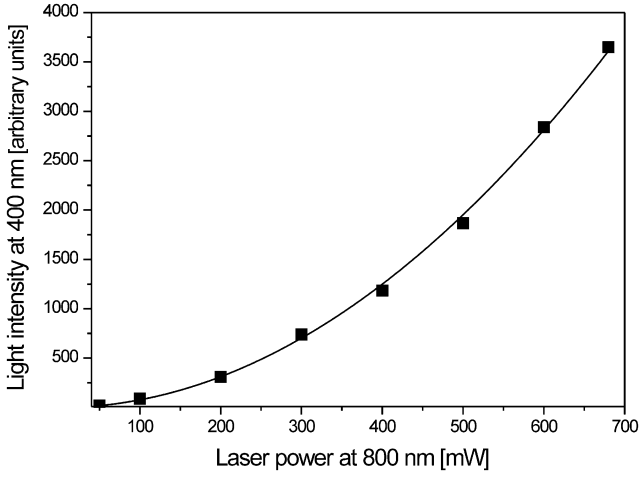

Fig. 12. The intensity dependence of SHG for powdered **4-atox** measured at 800 nm (points). The solid line is the theoretical quadratic dependence.

4. Conclusion

Three novel compounds **4-atox**, **4-atsuc** and **4-atadip** were prepared and their crystal structures were solved by the method of X-ray diffraction in this paper. **4-atox** is an organic salt, whose crystal structure consists of periodically alternating layers formed by chains of hydrogen oxalate anions connected by O–H···O hydrogen bonds. These layers are interconnected by **4-at(1+)** cations via N–H···O hydrogen bonds. The crystal structure of the **4-atsuc** adduct (1:1) is formed by zig-zag chains of **4-at** molecules, connected by N–H···N hydrogen bonds, and isolated molecules of succinic acid which interconnect these chains through O–H···N and N–H···O hydrogen bonds. Finally, the crystal structure of the **4-atadip** adduct (2:1) consists of pairs of parallel linear chains (mediated by N–H···N hydrogen bonds) of **4-at** molecules, which are interconnected by isolated adipic acid molecules via O–H···N and N–H···O hydrogen bonds. Neighbouring chains do not exhibit any H-bond contact between each other. Different protonisation of dicarboxylic acids in **4-atox**, **4-atsuc** and **4-atadip** compounds can be easily explained by the values of the dissociation constants at 298 K [48]. Oxalic acid is a much stronger acid ($pK_1 = 1.23$, $pK_2 = 4.19$), forming the hydrogen oxalate of **4-at(1+)**, than succinic ($pK_1 = 4.22$, $pK_2 = 5.70$) and adipic ($pK_1 = 4.44$, $pK_2 = 5.44$) acids, forming addition compounds with **4-at** under similar conditions.

The FTIR and FT Raman spectra of all three compounds were recorded and their interpretation is based on quantum chemical calculations of the isolated 4-amino-1,2,4-triazole molecule and its monocation.

The observed SHG efficiency (38% compared to KDP) together with optical transparency and thermal stability indicate the possibility of utilisation of **4-atox** crystals as a novel NLO material.

Acknowledgements

This work was financially supported by the Grant Agency of Charles University in Prague (Grant No. 337/2005/B-Ch) and is part of the long term Research Plan of the Ministry of Education of the Czech Republic No. MSM0021620857.

References

[1] V.P. Sinditskii, V.I. Sokol, A.E. Fogel'zang, M.D. Dutov, V.V. Serushkin, M.A. Porai-Koshits, B.S. Svetlov, Zh. Neorg. Khim. 32 (1987) 1950.
[2] J.G. Haasnoot, Coord. Chem. Rev. 200–202 (2000) 131.
[3] M.H. Klingele, S. Brooker, Coord. Chem. Rev. 241 (2003) 119.
[4] U. Beckmann, S. Brooker, Coord. Chem. Rev. 245 (2003) 17.
[5] R.N. Muller, L.V. Elst, S. Laurent, J. Am. Chem. Soc. 125 (2003) 8405.
[6] Y. Muracami, T. Komatsu, N. Kojima, Synthetic Met. 103 (1999) 2157.
[7] S. Komeda, S. Bombard, S. Perrier, J. Reedijk, J. Kozelka, J. Inorg. Biochem. 96 (2003) 357.
[8] W. Li, Q. Wu, Y. Yu, M. Luo, L. Hu, Y. Gu, F. Niu, J. Hu, Spectrochim. Acta A60 (2004) 2343.
[9] B. Mernari, H. Elattari, M. Traisnel, F. Bentiss, M. Langrenée, Corros. Sci. 40 (1998) 391.
[10] F. Bentiss, M. Langrenée, M. Traisnel, J.C. Hornez, Corros. Sci. 41 (1999) 789.
[11] X. Mei, Ch. Wolf, Eur. J. Org. Chem. 21 (2004) 4340.
[12] S. Baitalik, B. Dutta, K. Nag, Polyhedron 23 (2004) 913.
[13] C. Di Pietro, S. Serroni, S. Campagna, M.T. Gandolfi, R. Ballardini, S. Fanni, W.R. Browne, G. Vos Johannes, Inorg. Chem. 41 (11) (2002) 2871.
[14] Z. Kotler, R. Hierle, D. Josse, J. Zyss, R. Masse, J. Opt. Soc. Am. B 9 (1992) 534.
[15] J. Zyss, R. Masse, M. Bagieu-Beucher, J.P. Levy, Adv. Mater. 5 (1993) 20.
[16] N. Horiuchi, F. Lefaucheux, A. Ibanez, D. Josse, J. Zyss, J. Opt. Soc. Am. B 19 (2002) 1830.
[17] I. Matulková, I. Němec, I. Císařová, P. Němec, Z. Mička, J. Mol. Struct. 834–836 (2007) 328.
[18] J. Zyss, J.F. Nicoud, M. Coquillay, J. Chem. Phys. 81 (9) (1984) 4160.

[19] V.R. Thalladi, S. Brasselet, H. Ch. Weiss, D. Bläster, A.K. Katz, H.L. Carrell, R. Boese, J. Zyss, A. Nangia, G.R. Desiraju, J. Am. Chem. Soc. 120 (1998) 2563.
[20] J. Zyss, S. Brasselet, V.R. Thalladi, G.R. Desiraju, J. Chem. Phys. 109 (1998) 658.
[21] M. Ravi, P. Gangopadhyay, D.N. Rao, S. Cohen, I. Agranat, T.P. Radhakrishnan, Chem. Mater. 10 (1998) 2371.
[22] V.R. Thalladi, R. Boese, S. Brasselet, I. Ledoux, J. Zyss, R.K.R. Jetti, G.R. Desiraju, Chem. Commun. (1999) 1639.
[23] G.R. Desiraju, J. Mol. Struct. 656 (2003) 5.
[24] C.B. Aakeröy, K.R. Seddon, Chem. Soc. Rev. 22 (6) (1993) 397.
[25] D. Xue, S. Zhang, J. Phys. Chem. Solids 57 (9) (1996) 1321.
[26] D. Xue, S. Zhang, J. Phys. Chem. A 101 (1997) 5547.
[27] F. Billes, H. Endrédi, G. Keresztury, J. Mol. Struct. (Teochem) 530 (2000) 183.
[28] M.H. Palmer, D. Christen, J. Mol. Struct. 705 (2004) 177.
[29] C. Castiglioni, M. Gussoni, M.D. Zoppo, G. Zerbi, Solid State Commun. 82 (1992) 13.
[30] P. Zuliani, M.D. Zoppo, C. Castiglioni, G. Zerbi, C. Andraud, T. Brotin, A. Collet, J. Phys. Chem. 99 (1995) 16242.
[31] B. Kirrtman, B. Champagne, J.M. André, J. Chem. Phys. 104 (1996) 4125.
[32] M.D. Zoppo, A. Lucotti, C. Bertarelli, G. Zerbi, Vib. Spectrosc. 42 (2007) 249.
[33] R.M. Herbert, J.A. Garrison, J. Org. Chem. 18 (1953) 872.
[34] D. Sanz, M.P. Torralba, S.H. Alarcón, R.M. Claramunt, C.F. Foces, J. Elguero, J. Org. Chem. 67 (2002) 1462.
[35] A. Altomare, M.C. Burla, M. Camalli, G. Cascarano, C. Giacovazzo, A. Guagliardi, G. Polidori, SIR97—J. Appl. Crystallogr. 27 (1994) 435.
[36] G.M. Sheldrick, SHELXL 97, Program for Refinement from Diffraction Data, University of Göttingen, Germany, Göttingen, 1997.
[37] Gaussian 98W, Revision A.11, M.J. Frisch, G.W. Trucks, H.B. Schlegel, G.E. Scuseria, M.A. Robb, J.R. Cheeseman, V.G. Zakrzewski, J.A. Montgomery, Jr., R.E. Stratmann, J.C. Burant, S. Dapprich, J.M. Millam, A.D. Daniels, K.N. Kudin, M.C. Strain, O. Farkas, J. Tomasi, V. Barone, M. Cossi, R. Cammi, B. Mennucci, C. Pomelli, C. Adamo, S. Clifford, J. Ochterski, G.A. Petersson, P.Y. Ayala, Q. Cui, K. Morokuma, P. Salvador, J.J. Dannenberg, D.K. Malick, A.D. Rabuck, K. Raghavachari, J.B. Foresman, J. Cioslowski, J.V. Ortiz, A.G. Baboul, B.B. Stefanov, G. Liu, A. Liashenko, P. Piskorz, I. Komaromi, R. Gomperts, R.L. Martin, D.J. Fox, T. Keith, M.A. Al-Laham, C.Y. Peng, A. Nanayakkara, M. Challacombe, P.M.W. Gill, B. Johnson, W. Chen, M.W. Wong, J.L. Andres, C. Gonzalez, M. Head-Gordon, E.S. Replogle, and J.A. Pople, Gaussian, Inc., Pittsburgh PA, 2001.
[38] GaussView, version 2.1, Gaussian, Inc., Pittsburgh PA, 2001.
[39] NIST Computational Chemistry Comparison and Benchmark Data-Base, NIST Standard Reference Database Number 101 Release 10, May 2004, Russell D. Johnson III (Ed.), <http://srdata.nist.gov/cccbdb/vibscalejust.asp>.
[40] G. Socrates, Infrared and Raman Characteristic Group Frequencies (Tables and Charts), John Wiley and sons, Baffins Lane, Chichester, West Sussex, England, 2001, p. 125.
[41] Ch. W. Bock, R.L. Redington, J. Chem. Phys. 85 (10) (1986) 5391.
[42] J. De Villepin, A. Novak, D. Bougeard, Chem. Phys. 73 (1982) 291.
[43] P. Tarakeshwar, S. Manogaran, J. Mol. Struct. (Teochem) 362 (1996) 77.
[44] A. Lautié, F. Froment, A. Novak, Spectrosc. Lett. 9 (1976) 289.
[45] A. Novak, Struct. Bond. 18 (1973) 177.
[46] J.P. Castaneda, G.S. Denisov, S.Y. Kucherov, V.M. Schreiber, A.V. Shurukhina, J. Mol. Struct. 660 (2003) 25.
[47] S.K. Kurtz, T.T. Perry, J. Appl. Phys. 39 (1968) 3798.
[48] The Combined Chemical Dictionary – Chemical Databases Online: <http://www.chemnetbase.com/scripts/ccdweb.exe>.
[49] A.L. Spek, J. Appl. Crystallogr. 36 (2003) 7.